JACS
ARTICLES
Published on Web 11/13/2008

MoS_2 Nanoribbons: High Stability and Unusual Electronic and Magnetic Properties

Yafei Li,[†] Zhen Zhou,*[,†] Shengbai Zhang,[‡] and Zhongfang Chen*[,‡,§]

Institute of New Energy Material Chemistry, Institute of Scientific Computing, Nankai University, Tianjin 300071, People's Republic of China, Department of Physics, Applied Physics, and Astronomy, Rensselaer Polytechnic Institute, Troy, New York 12180, and Department of Chemistry, Institute for Functional Nanomaterials, University of Puerto Rico, Rio Piedras Campus, San Juan, Puerto Rico 00931

Received July 17, 2008; E-mail: zhouzhen@nankai.edu.cn (Z.Z.); zhongfangchen@gmail.com (Z.C.)

Abstract: First-principles computations were carried out to predict the stability and magnetic and electronic properties of MoS_2 nanoribbons with either zigzag- or armchair-terminated edges. Zigzag nanoribbons show the ferromagnetic and metallic behavior, irrespective of the ribbon width and thickness. Armchair nanoribbons are nonmagnetic and semiconducting, and the band gaps converge to a constant value of ~0.56 eV as the ribbon width increases. The higher stability of MoS_2 nanoribbons, compared with the experimentally available triangular MoS_2 nanoclusters, invites the experimental realization of such novel ribbons in true nanoscale.

Introduction

One-dimensional (1-D) nanostructures, such as nanorods, nanotubes, nanowires, and nanobelts, have been of both fundamental and technological interest during the past two decades due to the interesting electronic and physical properties intrinsically associated with their low dimensionality and quantum confinement effect. Recently, graphene nanoribbons, thin strips of graphene or unrolled single-walled carbon nanotubes with nanometer-sized width, have been successfully synthesized.[1] This novel 1-D carbon nanomaterial holds extremely promising applications in future nanoscale electronic devices.[2−5] The electronic and magnetic properties of graphene nanoribbons have been intensively studied.[6−18] The tight-binding computations showed that H-terminated graphene nanoribbons with armchair edges are metallic if the ribbon width parameter $N_a = 3p - 1$ (where p is an integer), or otherwise semiconducting, while those with zigzag edges are all metallic independent of their width parameter N_z.[6−8] However, more accurate first-principles computations revealed that both varieties of ribbons have band gaps,[12−15] and the theoretically predicted inverse dependence of the energy gap on the nanoribbon width was confirmed experimentally.[16] Especially, those graphene nanoribbons with zigzag edges are characterized with the localized edge states and the corresponding flat energy bands at the Fermi level.[7,12] Recently, Louie et al.[17] predicted that the half-metallicity (the coexistence of metallic nature for electrons with one spin orientation and insulating nature for electrons with the other) in graphene nanoribbons can be realized under an external transverse electric field, while Yang et al.[18] predicted that edge-modified zigzag graphene nanoribbons can also be half-metal. The half-metallicity of graphene nanoribbons opens up an opportunity for spintronics devices.

As a kind of layered semiconducting material, molybdenum disulfide (MoS_2) has also attracted much research interest for

[†] Nankai University.
[‡] Rensselaer Polytechnic Institute.
[§] University of Puerto Rico.

(1) Novoselov, K. S.; Geim, A. K.; Morozov, S. V.; Jiang, D.; Zhang, Y.; Dubonos, S. V.; Grigorieva, I. V.; Firsov, A. A. *Science* **2004**, *306*, 666.
(2) For recent reviews, see: (a) Geim, A. K.; Novoselov, K. S. *Nat. Mater.* **2007**, *6*, 183. (b) Fukui, K.-I.; Kobayashi, Y.; Enoki, T. *Int. Rev. Phys. Chem.* **2007**, *26*, 609.
(3) Zhang, Y.; Tan, Y.; Stormer, H.; Kim, P. *Nature* **2005**, *438*, 201.
(4) Berger, C.; Song, Z.; Li, X.; Wu, X.; Brown, N.; Naud, C.; Mayou, D.; Li, T.; Hass, J.; Marchenkov, A. N.; Conrad, E. H.; First, P. N.; De Heer, W. A. *Science* **2006**, *312*, 1191.
(5) Novoselov, K. S.; Jiang, Z.; Zhang, Y.; Morozov, S. V.; Stormer, H. L.; Zeitler, U.; Maan, J. C.; Boebinger, G. S.; Kim, P.; Geim, A. K. *Science* **2007**, *315*, 1379.
(6) Fujita, M.; Wakabayashi, K.; Nakada, K.; Kusakabe, K. *J. Phys. Soc. Jpn.* **1996**, *65*, 1920.
(7) Nakada, K.; Fujita, M.; Dresselhaus, G.; Dresselhaus, M. S. *Phys. Rev. B* **1996**, *54*, 17954.
(8) (a) Wakabayashi, K.; Sigrist, M.; Fujita, M. *J. Phys. Soc. Jpn.* **1998**, *67*, 2089. (b) Wakabayashi, K.; Fujita, M.; Ajiki, H.; Sigrist, M. *Phys. Rev. B* **1999**, *59*, 8271.
(9) Kawai, T.; Miyamoto, Y.; Sugino, O.; Koga, Y. *Phys. Rev. B* **2000**, *62*, 16349.
(10) Kusakabe, K.; Maruyama, M. *Phys. Rev. B* **2003**, *67*, 092406.
(11) Yamashiro, A.; Shimoi, Y.; Harigaya, K.; Wakabayashi, K. *Phys. Rev. B* **2003**, *68*, 193410.
(12) Son, Y.-W.; Cohen, M. L.; Louie, S. G. *Phys. Rev. Lett.* **2006**, *97*, 216803.
(13) (a) Jiang, D. E.; Sumpter, B. G.; Dai, S. *J. Chem. Phys.* **2007**, *127*, 124703. (b) Jiang, D. E.; Sumpter, B. G.; Dai, S. *J. Chem. Phys.* **2007**, *126*, 134701. (c) Gao, X. F.; Zhou, Z.; Zhao, Y. L.; Nagase, S.; Zhang, S. B.; Chen, Z. F. *J. Phys. Chem. C* **2008**, *112*, 12677.
(14) Barone, V.; Hod, O.; Scuseria, G. E. *Nano Lett.* **2006**, *6*, 2748.
(15) Yang, L.; Park, C. H.; Son, Y. W.; Cohen, M. L.; Louie, S. G. *Phys. Rev. Lett.* **2007**, *99*, 186801.
(16) Han, M. Y.; Özyilmaz, B.; Zhang, Y.; Kim, P. *Phys. Rev. Lett.* **2007**, *98*, 206805.
(17) Son, Y.-W.; Cohen, M. L.; Louie, S. G. *Nature* **2006**, *444*, 347.
(18) Kan, E. J.; Li, Z. Y.; Yang, J. L.; Hou, J. G. *J. Am. Chem. Soc.* **2008**, *130*, 4224.

its excellent properties and potential applications.[19−21] Unlike graphite and layered hexagonal BN (h-BN), the monolayer of MoS_2 is composed of three atom layers: a Mo layer sandwiched between two S layers. The triple layers are stacked and held together through weak van der Waals (vdW) interaction. The tubular form of MoS_2[22−25] has been synthesized in Tenne's group shortly after the realization of its fullerene-like nanostructures, and its applications have been exploited.[25−29] Theoretically, Seifert et al.[30,31] performed density functional theory based tight-binding (DFTB) computations to investigate the structural and electronic properties of MoS_2 nanotubes. Armchair MoS_2 nanotubes are deduced to have a nonzero moderate band gap, and zigzag MoS_2 nanotubes possess a narrow direct band gap, implying the promising applications in optoelectronic and luminescent devices. Other MoS_2 nanostructures, such as nanoparticles, multiwalled nanotubes, and fibrous flocs, have also been realized experimentally.[32] Moreover, Helveg et al.[33] demonstrated that single-layered MoS_2 can grow on a reconstructed Au(111) substrate, which was observed through scanning tunneling microscopy (STM). The single-layered MoS_2 has a triangular shape and possesses up to two 1-D localized metallic edge states,[34] which is different from the semiconducting bulk MoS_2 and nanotubes. Recently, Zhang et al.[35] have detected dilute magnetism from MoS_2 nanofilms. Through density functional theory (DFT) computations on cluster models, they demonstrated that the magnetism mainly arises from the unsaturated atoms at the prismatic edge sites.

It is remarkable to achieve magnetism in nonmagnetic MoS_2 without introducing metal impurities. However, with increasing cluster size, the ratio of edge atoms vs the total number of atoms will decrease dramatically as well as the unit magnetic moment. Therefore, only weak magnetism can be observed from polycrystalline MoS_2 films. Recently, Botello-Méndez et al.[36] have reported that ZnO nanoribbons with zigzag-terminated edges exhibit magnetic behaviors independently of the ribbon width. The intensive studies of graphene and other nanoribbons inspired us to answer some urgent questions: Can single-layered MoS_2 be cut into 1-D nanoribbons to obtain a constant edge atom ratio? Actually, there have been several reports[37−40] on the synthesis of MoS_2 ribbons; however, the widths of those ribbons are in the microscale. Is it feasible to realize them in true nanoscale experimentally? What about the stability and electronic and magnetic properties of MoS_2 nanoribbons? In this work, we performed DFT computations to address the above issues.

Computational Methods

The models of MoS_2 nanoribbons are constructed by cutting a single-layered MoS_2 with the desired edges and widths. Following the previous convention of graphene nanoribbons,[6−18] the width parameter N_z (N_a) of MoS_2 nanoribbons is defined as the number of zigzag lines (dimmer lines) across the ribbon width. We considered zigzag ribbons with N_z up to 24 (width up to 6.43 nm) and armchair ribbons with N_a up to 35 (width up to 5.39 nm). The 1-D periodic boundary condition (PBC) was applied along the growth direction of the nanoribbons to simulate infinitely long nanoribbon systems. For both kinds of ribbons the supercell model contains two unit cells.

Our spin-polarized first-principles DFT computations were performed using a plane wave basis set with the projector-augmented plane wave (PAW)[41] to model the ion−electron interaction as implemented in the Vienna ab initio simulation package (VASP).[42] The generalized gradient approximation (GGA) with the PW91[43] functional and a 360 eV cutoff for the plane-wave basis set were adopted in all the computations. The following electronic states were treated as valence: Mo, $4p^6 5s^1 4d^5$; S, $3s^2 3p^4$. Our supercells are large enough to ensure that the vacuum space is at least 10 Å, so that the interaction between nanoribbons and their periodic images can be safely avoided. Five Monkhost−Pack special k points were used for sampling the 1-D Brillouin zone, and the convergence threshold was set as 10^{-4} eV in energy and 10^{-3} eV/Å in force. The positions of all the atoms in the supercell were fully relaxed during the geometry optimizations. On the basis of the equilibrium structures, 21 k points were then used to compute the electronic band structures.

Results and Discussion

Geometries and Magnetic Properties. First, we optimized the structure of a single MoS_2 layer (Figure S1, Supporting Information). Mo and S atoms are linked covalently in the triple layers. The lengths of the Mo−S bonds are uniformly 2.41 Å, Mo−S−Mo (or S−Mo−S) bond angles are 82.31°, and the

(19) Paskach, Y. J.; Schrader, G. L.; McCarley, R. E. *J. Catal.* **2002**, *211*, 285.
(20) Bernede, J. C.; Pouzet, J.; Gourmelon, E.; Hadouda, H. *Synth. Met.* **1999**, *99*, 45.
(21) Muratore, C.; Voevodin, A. A. *Surf. Coat. Technol.* **2006**, *201*, 4125.
(22) Tenne, R.; Margulis, L.; Genut, M.; Hodes, G. *Nature* **1992**, *360*, 444.
(23) Margulis, L.; Salitra, G.; Tenne, R.; Tallanker, M. *Nature* **1993**, *365*, 113.
(24) Tenne, R.; Homyonfer, M.; Feldman, Y. *Chem. Mater.* **1998**, *10*, 3225.
(25) (a) For recent reviews, see: Tenne, R.; Remškar, M.; Enyashin, A.; Seifert, G. *Top. Appl. Phys.* **2008**, *111*, 631. (b) Tenne, R. *Nat. Nanotechnol.* **2006**, *1*, 103. (c) Tenne, R. *J. Mater. Res.* **2006**, *21*, 2726. (d) Remškar, M. *Adv. Mater.* **2004**, *16*, 1497.
(26) Chen, J.; Kuriyama, N.; Yuan, H. T.; Takeshita, H. T.; Sakai, T. *J. Am. Chem. Soc.* **2001**, *123*, 11813.
(27) Dominko, R.; Arčon, D.; Mrzel, A.; Zorko, A.; Cevc, P.; Venturini, P.; Gaberscek, M.; Remškar, M.; Mihailovic, D. *Adv. Mater.* **2002**, *14*, 1531.
(28) Chen, J.; Li, S. L.; Xu, Q.; Tanaka, K. *Chem Commun.* **2002**, 1722.
(29) Kis, A.; Mihailovic, D.; Remškar, M.; Mrzel, A.; Jesih, A.; Piwonski, I.; Kulik, A. J.; Benoit, W.; Forro, L. *Adv. Mater.* **2003**, *15*, 733.
(30) Seifert, G.; Terrones, H.; Terrones, M.; Jungnickel, G.; Frauenheim, T. *Phys. Rev. Lett.* **2000**, *85*, 146.
(31) For recent reviews on theoretical studies on MoS_2 and other inorganic nanotubes, see: (a) Seifert, G.; Köhler, T.; Tenne, R. *J. Phys. Chem. B* **2002**, *106*, 2497. (b) Enyashin, A. N.; Gemming, S.; Seifert, G. *Springer Ser. Mater. Sci.* **2007**, *93*, 33.
(32) Li, X. L.; Li, Y. D. *J. Phys. Chem. B* **2004**, *108*, 13893.
(33) Helveg, S.; Lauritsen, J. V.; Lægsgaard, E.; Stensgaard, I.; Nørskov, J. K.; Clausen, B. S.; Topsøe, H.; Besenbacher, F. *Phys. Rev. Lett.* **2000**, *84*, 951.
(34) Bollinger, M. V.; Lauritsen, J. V.; Jacobsen, K. W.; Nørskov, J. K.; Helveg, S.; Besenbacher, F. *Phys. Rev. Lett.* **2001**, *87*, 196803.
(35) Zhang, J.; Soon, J. M.; Loh, K. P.; Yin, J. H.; Ding, J.; Sullivian, M. B.; Wu, P. *Nano Lett.* **2007**, *7*, 2370.
(36) Botello-Méndez, A. R.; López-Urías, F.; Terrones, M.; Terrones, H. *Nano Lett.* **2008**, *8*, 1562.
(37) (a) Ballif, C.; Regula, M.; Remškar, M.; Sanjinés, R.; Lévy, F. *Surf. Sci.* **1996**, *366*, L703. (b) Remškar, M.; Škraba, Z.; Regula, M.; Ballif, C.; Sanjinés, R.; Lévy, F. *Adv. Mater.* **1998**, *10*, 246. (c) Remškar, M.; Škraba, Z.; Cléton, F.; Sanjinés, R.; Lévy, F. *Surf. Rev. Lett.* **1998**, *5*, 423.
(38) (a) Li, Q.; Newberg, J. T.; Walter, E. C.; Hemminger, J. C.; Penner, R. M. *Nano Lett.* **2004**, *4*, 277. (b) Li, Q.; Walter, E. C.; van der Veer, W. E.; Murray, B. J.; Newberg, J. T.; Bohannan, E. W.; Switzer, J. A.; Hemminger, J. C.; Penner, R. M. *J. Phys. Chem. B* **2005**, *109*, 3169.
(39) Novoselov, K. S.; Jiang, D.; Schedin, F.; Booth, T. J.; Khotkevich, V. V.; Morozov, S. V.; Geim, A. K. *Proc. Natl. Acad. Sci. U.S.A.* **2005**, *102*, 10451.
(40) Nora Elizondo-Villarreal, N.; Velázquez-Castillo, R.; Galván, D. H.; Camacho, A.; Jose-Yacamán, M. *Appl. Catal., A* **2007**, *328*, 88.
(41) Blochl, P. E. *Phys. Rev. B* **1994**, *50*, 17953.
(42) Kresse, G.; Hafner, J. *Phys. Rev. B* **1993**, *47*, 558.
(43) Perdew, J. P.; Chevary, J. A.; Vosko, S. H.; Jackson, K. A.; Pederson, M. R.; Singh, D. J.; Fiolhais, C. *Phys. Rev. B* **1992**, *46*, 6671.

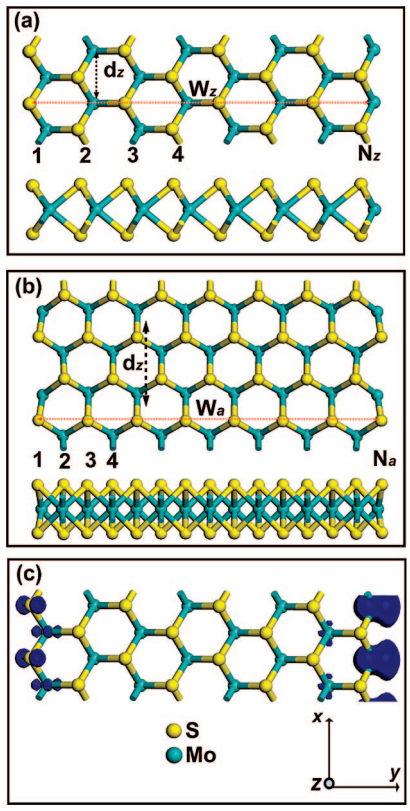

Figure 1. Top and side views of geometric structures of (a) 8-$ZMoS_2$NR and (b) 15-$AMoS_2$NR. The ribbon width and 1-D unit cell distance are denoted by W_z (W_a) and d_z (d_a), respectively. (c) Spatial spin distribution (up−down) of 8-$ZMoS_2$NR. MoS_2 nanoribbons are extended periodically along the x direction.

thickness of the triple layer is 3.13 Å. The computed binding energy is 5.20 eV per atom, and the single-layered MoS_2 is semiconducting with a direct band gap of 1.69 eV at the Γ point on the basis of the DFT-PW91 level. Our computational results achieve good agreement with previous studies.[30,34,35]

Two kinds of MoS_2 nanoribbons can be distinguished according to the different directions of termination: zigzag and armchair. Figure 1 displays the optimized geometries of two MoS_2 nanoribbons: (a) the 8-zigzag MoS_2 nanoribbon ($ZMoS_2$NR) and (b) the 15-armchair MoS_2 nanoribbon ($AMoS_2$NR), with widths of 20.34 and 22.40 Å, respectively. After full relaxation, the triple-layer networks are well kept at both ribbons, though the Mo−S bond lengths are changed: for the 8-$ZMoS_2$NR, the Mo−S bond lengths are 2.41, 2.42, and 2.45 Å in the inner sites and 2.37 and 2.39 Å in the Mo-terminated and S-terminated edges, respectively. For the 15-$AMoS_2$NR, the edge S atoms tend to shift outward slightly; the Mo−S bond lengths are 2.39, 2.41, and 2.44 Å in the inner sites and 2.29 Å in the two edges.

During the structure optimization, we have carried out both spin-unpolarized and spin-polarized computations to determine the ground state of MoS_2 nanoribbons. For armchair MoS_2 nanoribbons, spin-polarized total energies are less favorable than spin-unpolarized ones, indicating that armchair MoS_2 nanoribbons have a nonmagnetic ground state. However, zigzag MoS_2 nanoribbons have a ferromagnetic ground state, since we obtained an energy difference between their spin-unpolarized and spin-polarized total energies. Table 1 shows the computed energy difference (ΔE) between spin-polarized and spin-unpolarized states and total magnetic moments (**M**) per unit cell for a series of zigzag MoS_2 nanoribbons ($N_z = 5-10, 24$). 5-$ZMoS_2$NR has the lowest ΔE (29.88 meV) and total magnetic moment (0.733 μ_B), while 24-MoS_2NR has the highest ΔE (57.30 meV) and total magnetic moment (0.879 μ_B). Both ΔE and the total magnetic moment increase with increasing ribbon width. Especially, the considerable ΔE indicates that the ferromagnetic state of MoS_2 nanoribbons is rather stable. To get further insight and clarity of the magnetism of $ZMoS_2$NRs, we have computed the spatial spin distribution of 8-$ZMoS_2$NR. As shown in Figure 1c, the unpaired spin mainly concentrates on the edge Mo and S atoms, and the inner Mo atoms also contribute a small amount of unpaired spin. The unsaturated edge atoms should be responsible for the magnetic behavior of zigzag MoS_2 nanoribbons since the coordination of these atoms is different from that of the inner atoms. Distinct to zigzag ZnO nanoribbons[36] whose magnetism is only contributed by oxygen edge and zigzag graphene nanoribbons[12] whose two edges are antiferromagnetically coupled, the magnetism of our zigzag MoS_2 ribbons arises from both edges which are ferromagnetically coupled. Moreover, according to our computational results, the H-terminated zigzag MoS_2 nanoribbons (the edge S and Mo atoms are saturated with one and two H atoms, respectively) still have a ferromagnetic ground state, but the magnetism is weaker. For example, the total magnetic moment of 8-$ZMoS_2$NR decreases from 0.768 to 0.643 μ_B due to the H termination. H termination cannot remove the magnetism of zigzag MoS_2 nanoribbons since the edge atoms do not recover to the same state as that of inner atoms due to the H termination.

Table 1. Energy Difference (ΔE) between Spin-Polarized and Spin-Unpolarized States and Total Magnetic Moments (**M**) per Unit Cell for a Series of Zigzag MoS_2 Nanoribbons ($N_z = 5-10, 24$)[a]

N_z	ΔE (meV)	**M** (μ_B)
5	−29.88	0.733 (0.147)
6	−32.30	0.751 (0.125)
7	−35.24	0.764 (0.109)
8	−35.62	0.769 (0.096)
9	−36.80	0.772 (0.086)
10	−38.76	0.792 (0.079)
24	−57.30	0.879 (0.037)

[a] The values in parentheses are the unit magnetic moment per MoS_2 molecular formula.

For comparison, we also computed the magnetic properties of bulk MoS_2 and a single layer, which are both nonmagnetic, similar to the previous report.[35] The unit magnetic moment of MoS_2 nanoribbons (magnetic moment per MoS_2 molecular formula) decreases gradually with increasing ribbon width, implying that the magnetism of MoS_2 zigzag nanoribbons gets weaker and weaker as the ribbon width increases and disappears in the infinitely single-layered MoS_2 and bulk. This is because the magnetic behavior in MoS_2 nanoribbons results from the unsaturated edge atoms, and the ratio of edge atoms vs total atoms (given by $1/N_z$) decreases dramatically as the ribbon width increases. However, as long as the ribbon width is in the nanoscale, the magnetism of zigzag MoS_2 ribbons is always expectable.

Electronic Properties. The spin-resolved band structure of 8-$ZMoS_2$NR and spin-unpolarized band structure of 15-$AMoS_2$NR are presented in Figure 2. For comparison, we have also computed the band structures of (10,0) and (7,7) MoS_2 nanotubes since zigzag and armchair nanoribbons can be obtained by unfolding armchair and zigzag nanotubes, respec-

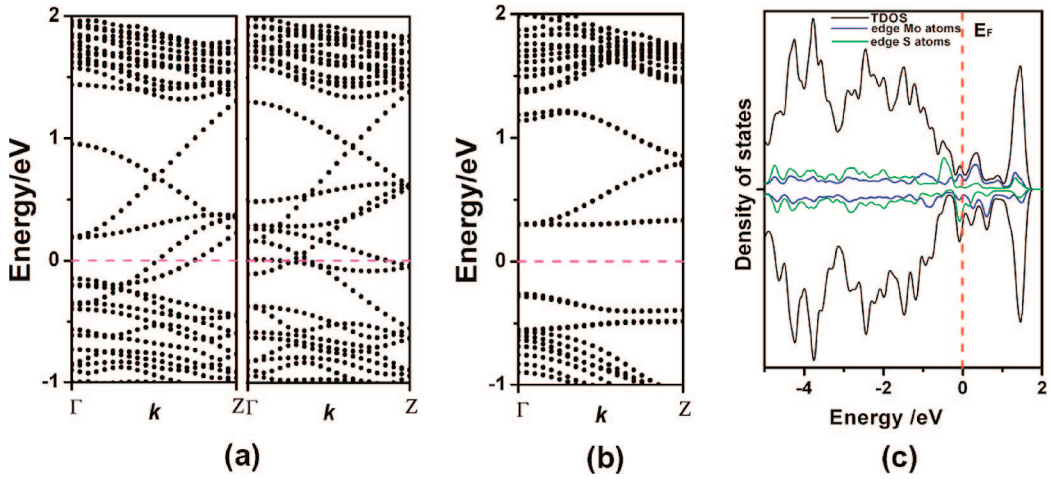

Figure 2. (a) Computed spin-polarized band structure for 8-ZMoS$_2$NR (left, majority spin; right, minority spin). (b) Computed band structure of 15-AMoS$_2$NR. (c) TDOS and LDOS for 8-ZMoS$_2$NR (top, majority spin; bottom, minority spin).

tively. Both zigzag and armchair MoS_2 nanotubes are semiconducting and have a spin-unpolarized ground state, similar to Seifert et al.'s report.[30] The (10,0) MoS_2 tube has a direct band gap of 0.31 eV, and the (7,7) nanotube has a direct gap of 1.13 eV at the Γ point and an indirect band gap of 0.44 eV (see Figure S2, Supporting Information). However, the electronic properties of zigzag MoS_2 nanoribbons are quite different from those of armchair nanotubes. As shown in Figure 2a, the majority spin bands and minority spin bands are asymmetric for 8-ZMoS$_2$NR, and both spin channels show a metallic feature: up to two energy levels in each spin channel cross the Fermi level and close the band gap. Also, this metallic behavior is independent of the ribbon width since the zigzag MoS_2 nanoribbons studied (including 24-ZMoS$_2$NR) are all metallic. This metallic behavior reminds us of the 1-D metallic channels in single-layered MoS_2.[34] To get more information about the characteristic metallic bands, we have computed the total density of states (TDOS) and local density of states (LDOS) of 8-ZMoS$_2$NR (Figure 2c). The states near the Fermi levels in both spin channels are dominated with the 4d electrons of edge Mo atoms and 3p electrons of edge S atoms.

In contrast, armchair MoS_2 nanoribbons inherit the semiconducting character of zigzag MoS_2 nanotubes. As shown in Figure 2b, 15-AMoS$_2$NR is a typical semiconductor with a direct band gap of 0.56 eV. The dispersions of both the top valence band and especially the bottom conduction band are very flat. Moreover, we have computed the band structures of a series of armchair MoS_2 nanoribbons, and their band gaps as a function of ribbon width are presented in Figure 3. All armchair MoS_2 nanoribbons considered here are semiconducting, and their electronic properties are weakly dependent on the ribbon width. Band gap oscillations are observed for the narrow ribbons, and those ribbons of $N_a = 3p - 1$ (where p is an integer) have larger band gaps than the neighboring two ribbons. However, as the width increases, the band gaps finally converge to a constant value of ~0.56 eV. The trend is quite similar to that of armchair BN nanoribbons.[44,45] To confirm this trend, we have computed 35-AMoS$_2$NR (width 5.39 nm), which also shows a band gap of 0.56 eV. This value is much smaller than that of single-layered MoS_2 (1.69 eV) since the edge atoms of nanoribbons introduce new flat energy levels at both valence and conduction band edges, narrowing the band gap accordingly. Overall, the uniform electronic properties may be a key advantage for their applications to nanotechnology.

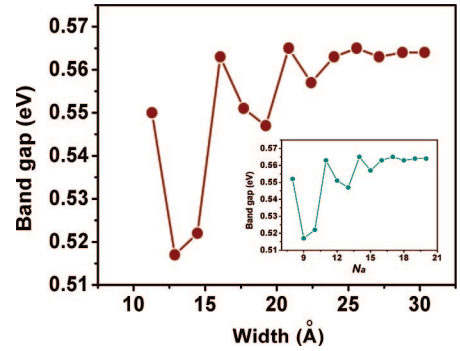

Figure 3. Variation of energy band gaps for a series of armchair MoS_2 nanoribbons ($8 \le N_a \le 20$) as a function of the ribbon width. The inset is the relationship of band gaps of armchair MoS_2 nanoribbons as a function of N_a.

Thickness Effect on Magnetic and Electronic Properties. Since the experimentally synthesized nanoribbons are assembled by several layers, we also investigated the effect of the thickness on the magnetic and electronic properties of zigzag MoS_2 nanoribbons. Here 5-ZMoS$_2$NR (width 1.20 nm) was chosen as an example for the consideration of computational feasibility. Up to four triple layers were placed on top of each other with an ABA sequence. Botello-Méndez et al.[36] reported that, in ZnO nanoribbons, edge atoms of the top layer can form covalent bonds with edge atoms of the bottom layer, and the magnetism and metallicity diminish when the number of layers is even. In contrast, for MoS_2 nanoribbons with more layers, there is no strong interaction between neighboring triple layers. In Figure 4a we show the optimized structure of a four-layered MoS_2 nanoribbon, the four triple layers are held together through weak vdW interaction, and the average separation between two neighboring layers is around 3.20 Å. (slightly larger than the experimental bulk value of 2.98 Å,[46] due to the underestimate

(44) Du, A.; Smith, S. C.; Lu, G. *Chem. Phys. Lett.* **2007**, *447*, 181.
(45) Park, C. H.; Louie, S. G. *Nano Lett.* **2008**, *8*, 2200.
(46) Böker, Th.; Severin, R.; Müller, A.; Janowitz, C.; Manzke, R.; Voss, D.; Krüger, P.; Mazur, A.; Pollmann, J. *Phys. Rev. B* **2001**, *64*, 235305.

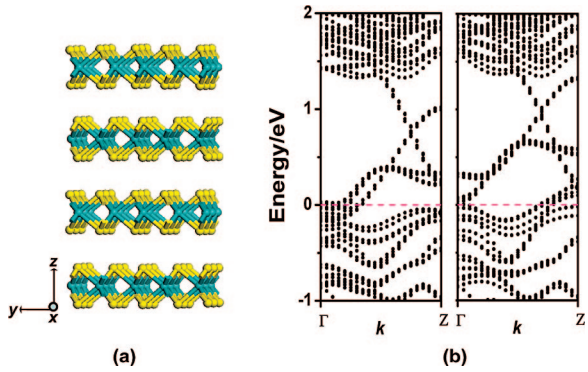

Figure 4. (a) Optimized structure of four-layered 5-ZMoS$_2$NR constructed by stacking individual MoS_2 sheets. (b) Computed band structure (left, majority spin; right, minority spin) of four-layered 5-ZMoS$_2$NR.

Table 2. Energy Difference (ΔE) between Spin-Polarized and Spin-Unpolarized States and Magnetic Moment (**M**) per Unit Cell of 5-ZMoS$_2$NR with Different Layer Numbers[a]

n	ΔE (meV)	**M** (μB)
1	−29.9	0.733 (0.147)
2	−70.6	1.696 (0.170)
3	−125.1	2.559 (0.171)
4	−144.0	3.008 (0.150)

[a] The values in parentheses are the unit magnetic moment per MoS_2 molecular formula.

of vdW interaction by GGA). The computed energy difference (ΔE) between spin-polarized and spin-unpolarized states and the magnetic moment (**M**) for multilayer MoS_2 nanoribbons are presented in Table 2. The magnetism is found in all the MoS_2 nanoribbons with more layers, whether the layer number is odd or even, and the computed ΔE and magnetic moments increase with increasing layer number. However, the unit magnetic moments do not change much as the layer number increases. When the ribbon width is kept in the nanoscale, the magnetic properties are reserved even at greater thickness, since the ratio of edge atoms vs total atoms is constant. The spin-resolved band structure for four-layered ribbons is shown in Figure 4b. Both the spin channels show a metallic feature. Therefore, we can safely conclude that zigzag MoS_2 nanoribbons can always keep the magnetic and metallic behaviors, irrespective of their width and thickness. The much weaker interlayer interaction in MoS_2 nanoribbons, compared with that in wurtzite ZnO nanoribbons, contributes to the different structural and magnetic evolution of ZnO and MoS_2 multilayer nanoribbons.

Stabilities of MoS_2 Nanoribbons. The stability of MoS_2 nanoribbons is quite important since it can determine whether this nanostructure can be realized experimentally. To estimate the stability, we have computed the binding energy per atom for both zigzag and armchair MoS_2 nanoribbons as a function of the ribbon width and compared it with that of triangular MoS_2 nanoclusters, which have been synthesized successfully.[47] Here the binding energy, E_b, is defined as $E_b = (nE_{Mo} + mE_S - E_{Mo_nS_m})/(n + m)$, in which E_{Mo}, E_S, and $E_{Mo_nS_m}$ are the respective energies of Mo, S, and Mo_nS_m. n and m are the number of Mo and S atoms, respectively. The stability of different ribbons and clusters can be evaluated with binding energies; those with larger binding energies are more stable.

(47) Lauritsen, J. V.; Kibsgaard, J.; Helveg, S.; Topsøe, H.; Clausen, B. S.; Lægsgaard, E.; Besenbacher, F. *Nat. Nanotechnol.* **2007**, *2*, 53.

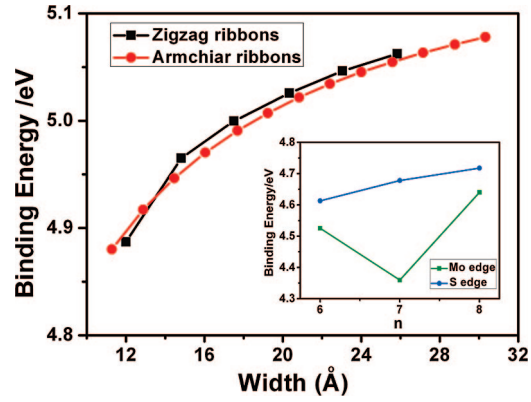

Figure 5. Binding energy of ZMoS$_2$NRs ($5 \le N_z \le 10$) and AMoS$_2$NRs ($8 \le N_a \le 20$) as a function of the ribbon width. The inset is the variation in the binding energies of several triangular MoS_2 nanoclusters terminated by a Mo edge or S edge (size range $n = 6-8$). The parameter n denotes the number of Mo atoms at the edge of the MoS_2 triangle. See Figure S4 (Supporting Information) for the configurations of the triangular MoS_2 nanoclusters.

As shown in Figure 5, the binding energies increase monotonically with increasing ribbon widths for both zigzag and armchair MoS_2 nanoribbons. The binding energies of zigzag ribbons are slightly higher than those of armchair ribbons with comparable widths. Especially, for those ribbons with the same number of atoms per unit, the binding energies of zigzag ribbons are much higher than those of armchair ribbons, such as 8-ZMoS$_2$NR (5.00 eV) vs 8-AMoS$_2$NR (4.88 eV). This demonstrates vigorously that zigzag MoS_2 nanoribbons are energetically more favorable than armchair nanoribbons. Moreover, both zigzag and armchair MoS_2 nanoribbons are more stable than triangular MoS_2 nanocluters. For example, the least stable nanoribbon in our studies, 5-ZMoS$_2$NR, even has a larger binding energy than the triangular MoS_2 nanocluster with an equilateral side consisting of eight atoms ($n = 8$; see Figure S4, Supporting Information[47]). As triangular MoS_2 nanoclusters have been synthesized,[47] and microscale MoS_2 nanoribbons have been produced,[37−40] we strongly believe that further efforts of experimental peers will realize the rather stable MoS_2 ribbons in true nanoscale in the very near future.

Conclusion

In summary, we presented the first theoretical investigations on the stability and electronic and magnetic properties of MoS_2 nanoribbons with zigzag- and armchair-terminated edges. Zigzag nanoribbons exhibit magnetic behavior, and the magnetic moment mainly concentrates on the edge atoms; in contrast, armchair nanoribbons have nonamagnetic ground states. The electronic band computations demonstrate that zigzag MoS_2 nanoribbons are metallic while armchair nanoribbons are semiconducting and the band gap converges to a constant value of 0.56 eV with increasing ribbon width. Zigzag nanoribbons with multiple layers still keep magnetic and metallic character. Overall, zigzag nanoribbons are more stable than armchair nanoribbons, and both zigzag and armchair MoS_2 nanoribbons are more stable than the experimentally available MoS_2 nanoclusters. This high stability of MoS_2 nanoribbons strongly suggests that they are viable experimentally. Combined with other superior properties of molybdenum disulfide, such as resistance to oxidation and catalytic activity,[47] MoS_2 nanoribbons will not only diversify the renown MoS_2 nanostructure

family, but also provide many new opportunities in various fields such as nanoelectronics, nanotribology, and catalysis. We believe that MoS_2 nanoribbons can be realized in true nanoscale experimentally in the very near future, and the present theoretical results will promote further experimental and theoretical investigations on MoS_2 and other fascinating inorganic nanoribbons.

Acknowledgment. Support in China by the NSFC (Grants 20873067 and 50502021) and the SRF for ROCS, SEM and in the United States by NSF Grant CHE-0716718, the US Environmental Protection Agency (EPA Grant No. RD-83385601), the Institute for Functional Nanomaterials (NSF Grant 0701525), RPI Startup Fund (146316), and DOE/OS/BES (Contract No. DEAC36-99GO10337) is gratefully acknowledged. We thank Prof. Jijun Zhao (Dalian University of Technology) for providing us the structure files of MoS_2 nanotubes. We also thank the anonymous reviewers for valuable suggestions. This paper is dedicated to Prof. Panwen Shen.

Supporting Information Available: Optimized geometries, energies, and computed band structures of MoS_2 single layers, nanoribbons, nanoclusters, and nanotubes. This material is available free of charge via the Internet at http://pubs.acs.org.

JA805545X